Nuclear Instruments and Methods in Physics Research A 1059 (2024) 169011

Contents lists available at ScienceDirect

Nuclear Inst. and Methods in Physics Research, A

journal homepage: www.elsevier.com/locate/nima

Ionising radiation effects in a soft X-ray CMOS image sensor

Charles Townsend-Rose *, Thomas Buggey, James Ivory, Konstantin D. Stefanov, Andrew D. Holland

Centre for Electronic Imaging, The Open University, Walton Hall, Milton Keynes, MK7 6AA, UK

A R T I C L E   I N F O

Keywords:
CMOS image sensor
X-ray detectors
Radiation damage
Total ionising dose (TID)

A B S T R A C T

CIS221-X is a prototype monolithic CMOS image sensor, optimised for soft X-ray astronomy and developed for the proposed ESA THESEUS mission. A significant advantage of CMOS technology is its resistance to radiation damage. To assess this resistance, four backside-illuminated CIS221-X detectors have been irradiated up to a total ionising dose of 113 krad at the ESA ESTEC ^{60}Co facility. Using unirradiated readout electronics, the performance of each sensor has been measured before and after irradiation. The gain, readout noise and dark current are shown to increase, while the image lag remains unchanged. These measurements are compared to that of similar CMOS image sensors and a possible physical explanation is provided for each result.

1. Introduction

CIS221-X is a prototype soft X-ray CMOS image sensor [1], developed for the proposed ESA THESEUS mission [2]. Built on 35 μm thick, high-resistivity epitaxial silicon, the CIS221-X pinned photodiode (PPD) pixels feature deep depletion extension (DDE) implants which facilitate over-depletion by reverse substrate bias [3]. The 2048 × 2048 pixel array is split into 4 equally sized regions: 3 variants of 40 μm pitch square pixels and one of 10 μm pitch square pixels. All 40 μm pixels feature an addition pinning implant which concentrates charge towards the transfer gate during integration. For the 40 μm 'Variant #2' pixels, the additional pinning implant has a novel 'Christmas Tree' shape while the 'Variant #3' pixels have a larger transfer gate. An optical-light blocking filter (OBF) has been applied to half of the CIS221-X image area, covering half of each pixel region.

With the exception of dark current (which is subject to on-going investigation), the initial CIS221-X electro-optical performance [4] either meets or outperforms the beginning-of-life requirements for the THESEUS mission. To further qualify the image sensor's use in space it is necessary to assess its radiation hardness. Four backside-illuminated (BSI) CIS221-X devices have been irradiated up to the THESEUS end-of-life (EoL) total ionising dose (TID): ∼100 krad. The impact to electro-optical performance has been measured.

2. Methods

At the ESA ESTEC ^{60}Co facility, four BSI CIS221-X image sensors were irradiated with gamma-rays. As detailed in Table 1, three devices were irradiated biased (one of which has an OBF covering half the image area), one was irradiated unbiased with all pins grounded and another acted as a control. All irradiated devices were positioned between 87–110 cm from the ^{60}Co source and were covered by 6 mm of Perspex® to ensure charged-particle equilibrium. While at ambient temperature and pressure, three devices were exposed to ∼60 krad (∼$\frac{1}{2}$ EoL) TID while one was irradiated up to ∼110 krad (∼1 EoL) TID.

Using unirradiated readout electronics, the performance of each sensor was measured before irradiation, half-way through total irradiation and after total irradiation. The half-total-irradiation measurements were collected immediately after exposure. However, the total-irradiation measurements were not collected until approximately 45 days after the final irradiation, during which time the image sensors were stored at room temperature. All data were collected under vacuum ($<10^{-5}$ hPa), with the sensors over-depleted by reverse substrate bias (−20 V) and cooled to −40 °C.

3. Results and discussion

Similarly to the initial electro-optical characterisation [4], only the 'Variant #3' 40 μm pixel results are presented. There was no measurable change in the performance of the control device. For all irradiated devices, the conversion gain increased at a rate of ∼2.5%/100 krad. A similar result has been reported for the CIS115 CMOS image sensor and attributed to MOSFET threshold voltage shift [5]. For the CIS221-X, further testing would be required to confirm this as the cause of the increase in gain.

* Corresponding author.
E-mail address: Charles.Townsend-Rose@open.ac.uk (C. Townsend-Rose).

https://doi.org/10.1016/j.nima.2023.169011
Received 14 November 2023; Accepted 7 December 2023
Available online 12 December 2023

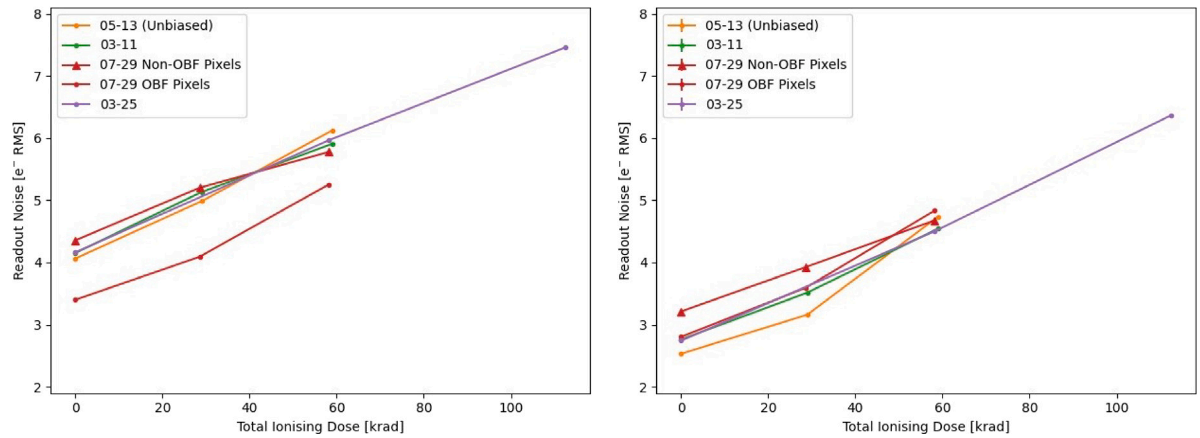

Fig. 1. CIS221-X readout noise measured at increasing total ionising dose inclusive (left) and exclusive (right) of a contribution from dark signal generated during readout. Data were collected with the image sensor cooled to −40 °C.

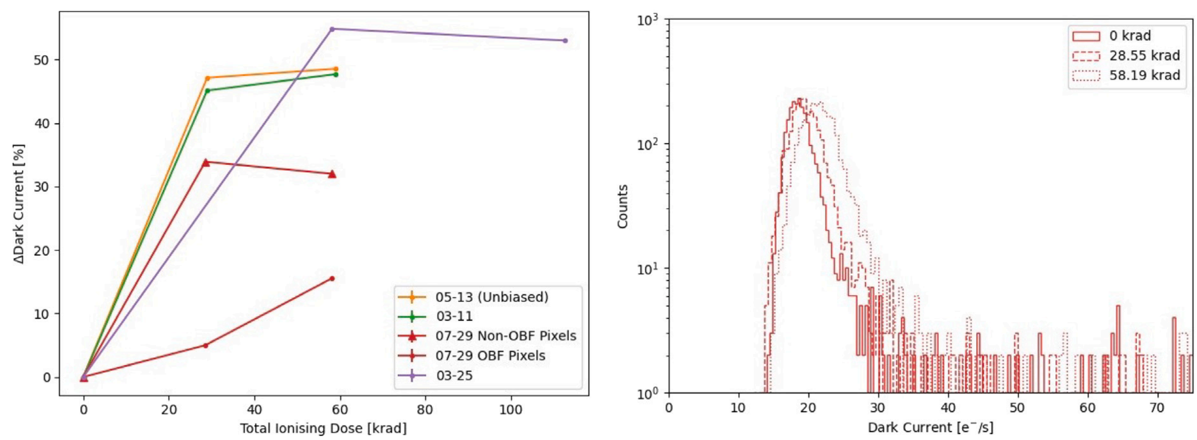

Fig. 2. CIS221-X dark current measured at increasing total ionising dose with the image sensor cooled to −40 °C. Left: Percentage change in dark current for increasing total ionising dose. Right: Dark current distribution of 07-29 OBF pixels at increasing total ionising dose.

3.1. Readout noise

Readout noise was measured using 50 dark frames. Dark current was not suppressed during data collection and therefore the initial measurement is a combination of both the noise from the on-chip readout electronics and the shot noise from the dark signal generated during readout. To decouple these two noise sources, the dark signal was subtracted using values derived from the dark current measurement (see Section 3.2). Fig. 1 shows the readout noise measured at increasing TID before (left) and after (right) dark signal subtraction. For all devices, the noise increased with TID at a similar rate; biasing and the presence of an OBF did not significantly influence the results. Prior to dark signal subtraction, the readout noise of the 07-29 non-OBF pixels is greater than that of the 07-29 OBF pixels. However, following dark signal subtraction, they report similar values. This suggests an offset in the dark current of the non-OBF and OBF pixels of this device. This phenomenon has been reported previously [4] and is subject to ongoing investigation.

The observed degradation of readout noise is again similar to measurements reported for a CIS115 CMOS image sensor [5]. In both cases, the increase in readout noise could be explained by the buildup of trapped charge and the generation of interface states in the MOSFET gate oxide and surrounding shallow trench isolation (STI) [6]. To verify this as the cause of degradation to the CIS221-X readout noise, further investigation would be necessary.

Table 1
BSI CIS221-X devices selected for radiation testing and the corresponding total ionising dose.

Serial no. 21094-	OBF/Non-OBF	Biased/Unbiased	Total ionising dose (EoL ~ 100 krad)
05-03	Non-OBF	–	–
05-13	Non-OBF	Unbiased	59.04 krad
03-11	Non-OBF	Biased	59.04 krad
07-29	OBF	Biased	58.19 krad
03-25	Non-OBF	Biased	112.51 krad

3.2. Dark current

Following exposure to ionising radiation, the dark current increased in all CIS221-X devices. Though no significant difference was seen in the results of the unbiased device, Fig. 2 (left) shows the performance of the 07-29 OBF pixels degraded less than that of the 07-29 non-OBF pixels. Further, for all but the 07-29 OBF pixels, the rate of degradation decreased significantly for the final irradiation measurement. Fig. 2 (right) shows the 07-29 OBF pixel dark current distribution uniformly increasing with TID. This uniformity was seen in all devices.

The degradation of CIS221-X dark current is comparable to that reported for a similar fully depleted PPD CMOS image sensor [7] for which the result was attributed to radiation-induced interface traps at the exposed edges of the STI. To verify this explanation for the CIS221-X, further testing would be required. The decreased rate of degradation for the final irradiation measurement is likely due to annealing that

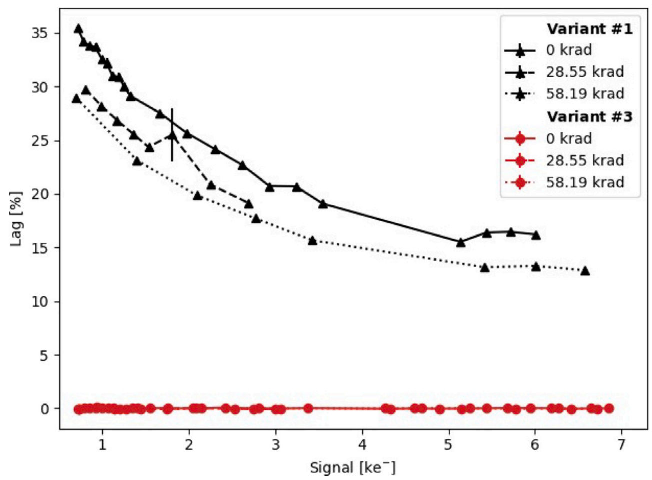

Fig. 3. Leading-edge image lag of the CIS221-X 'Variant #1' and 'Variant #3' 40 μm pixels expressed as a percentage of signal and measured at increasing total ionising dose. Results are from the 07-29 Non-OBF pixels and are representative of all devices tested.

occurred during the ~45 days between the final irradiation and the final dark current measurement, while the sensors were stored at room temperature. This could be confirmed through further data collection.

3.3. Image lag

The leading-edge image lag was measured using pulsed LED illumination. The lag performance of the 'Variant #1' and 'Variant #3' pixels (the subject of discussion so far) are shown in Fig. 3 as a percentage of signal. 'Variant #2' has been excluded for the sake of readability but reported similar results to the pixels of 'Variant #1': significant image lag before irradiation which then decreases with increasing TID. The 'Variant #3' pixels, which feature a larger transfer gate, have near-zero lag and show no measurable change following irradiation.

For pinned photodiode CMOS image sensor pixels, the main cause of image lag is the presence of a potential barrier or pocket between the photodiode and transfer gate. Following exposure to ionising radiation, positive charge trapped around these regions can lower or deepen any potential barrier or pocket [8]. The behaviour of the CIS221-X 'Variant #1/#2' pixels can then be explained by the presence of a significantly large potential barrier that has lowered following exposure to ionising radiation.

4. Conclusion

Four BSI CIS221-X devices have been irradiated up to the end-of-life total ionising dose for the THESEUS mission and the impact to electro-optical performance has been measured. The results have been compared to that of other CMOS image sensors and show a similar resistance to ionising radiation. These results therefore support the use of the CIS221-X for space applications, specifically the THESEUS mission.

The gain, readout noise and dark current increased with total ionising dose, while no measurable change was seen in the image lag. A possible physical explanation has been provided for each result. However, further work is necessary to confidently identify the specific mechanisms and locations of damage caused by ionising radiation.

Declaration of competing interest

There are no conflicts on interest.

Acknowledgment

The European Space Agency (ESA) under the E/0901-01 Technology Development Element "CMOS Image Sensor for X-ray Applications".

References

[1] J. Heymes, K. Stefanov, M. Soman, D. Gorret, D. Hall, K. Minoglou, D. Morris, J. Pratlong, T. Prod'homme, G. Tsiolis, A. Holland, Development of a photon-counting near-fano-limited X-ray CMOS image sensor for THESEUS' SXI, in: A.D. Holland, J. Beletic (Eds.), X-Ray, Optical, and Infrared Detectors for Astronomy IX, Vol. 11454, SPIE, International Society for Optics and Photonics, 2020, p. 114540I.

[2] L. Amati, P.T. O'Brien, D. Götz, E. Bozzo, A. Santangelo, The THESEUS space mission: updated design, profile and expected performances, in: J.-W.A. den Herder, S. Nikzad, K. Nakazawa (Eds.), Space Telescopes and Instrumentation 2020: Ultraviolet to Gamma Ray, Vol. 11444, SPIE, International Society for Optics and Photonics, 2021, p. 114442J.

[3] K.D. Stefanov, A.S. Clarke, J. Ivory, A.D. Holland, Design and performance of a pinned photodiode CMOS image sensor using reverse substrate bias, Sensors 18 (1) (2018).

[4] C. Townsend-Rose, T. Buggey, J. Ivory, K.D. Stefanov, L. Jones, O. Hetherington, A.D. Holland, T. Prod'homme, Electro-optical characterization of a CMOS image sensor optimized for soft X-ray astronomy, J. Astron. Telesc. Instrum. Syst. 9 (4) (2023) 046001.

[5] M.R. Soman, E.A.H. Allanwood, A.D. Holland, K. Stefanov, J. Pratlong, M. Leese, J.P.D. Gow, D.R. Smith, Electro-optic and radiation damage performance of the CIS115, an imaging sensor for the JANUS optical camera on-board JUICE, in: A.D. Holland, J. Beletic (Eds.), High Energy, Optical, and Infrared Detectors for Astronomy VII, Vol. 9915, SPIE, International Society for Optics and Photonics, 2016, 991515.

[6] J. Tan, B. Buttgen, A.J.P. Theuwissen, Analyzing the radiation degradation of 4-transistor deep submicron technology CMOS image sensors, IEEE Sens. J. 12 (6) (2012) 2278–2286.

[7] X. Meng, K.D. Stefanov, A.D. Holland, Proton and Gamma radiation effects on a fully depleted pinned photodiode CMOS image sensor, IEEE Trans. Nucl. Sci. 67 (6) (2020) 1107–1113.

[8] V. Goiffon, M. Estribeau, O. Marcelot, P. Cervantes, P. Magnan, M. Gaillardin, C. Virmontois, P. Martin-Gonthier, R. Molina, F. Corbiere, S. Girard, P. Paillet, C. Marcandella, Radiation effects in pinned photodiode CMOS image sensors: Pixel performance degradation due to total ionizing dose, IEEE Trans. Nucl. Sci. 59 (6) (2012).